Japanese Journal of Radiology (2026) 44:326–338
https://doi.org/10.1007/s11604-025-01895-2

ORIGINAL ARTICLE

Evaluation of the effect of peritumoral surrounding parenchymal features on radiological size measurement in breast cancer patients: a multicenter retrospective study (TR-BRC 2023-01)

Gul Esen[1,2] · Deniz Esin Tekcan Sanli[3] · Sibel Kul[4] · Pinar Balci[5] · Nermin Tuncbilek[6] · Levent Celik[7] · Yasemin Kayadibi[8] · Ayse Nur Oktay Alfatli[9] · Serap Gultekin[10] · Fusun Taskin[1,2] · Mustafa Erkin Aribal[1,2] · Emel Ozveri[11] · Fatma Tokat[12] · Aykut Teymur[4] · Isil Basara Akin[5] · Gulsah Ozdemir[6] · Davut Can Guner[13] · Seda Aladag Kurt[8] · Ozge Aslan[9] · Aydan Avdan Aslan[10] · Ebru Yilmaz[14] · Yasemin Nur Icten[15,16] · Ahmet Necati Sanli[15]

Received: 20 May 2025 / Accepted: 30 September 2025 / Published online: 25 October 2025

Abstract

Purpose To investigate the effects of radiological, clinical and histological features in the radiological assessment of tumor size in breast cancer, with a particular focus on the effect of surrounding parenchymal features (SPFs).

Method Patients with SPFs reported in the postoperative pathology reports were included in this retrospective multicenter study. Primary lesions were categorized as invasive, in situ (DCIS) or mixed (invasive + DCIS) carcinoma. Pathological tumor size was accepted as the gold standard and compared with tumor sizes measured on mammography (MMG), ultrasonography (US), and magnetic resonance imaging (MRI), according to the presence or absence of SPFs with or without atypia. The effects of other factors such as mammographic breast density, background parenchmal enhancement (BPE), lesion type, lesion size, tumor grade and patient age were also evaluated.

Results There were SPFs in 402/473 patients (85%); and 228 of them (56.7%) had high-risk lesions, of which 196 (48.8%) were lesions with atypia. Overall MRI had the best correlation levels in the presence of SPFs. US had agreement levels close to MRI for invasive and mixed tumors, but not for DCIS. Presence of atypical high-risk lesions decreased the correlation levels of MMG ($r=0.193$ vs $r=0.485$) and MRI ($r=0.220$ vs $r=0.679$) in DCIS, and of MRI in mixed tumors ($r=0.718$ vs $r=0.848$). Correlation levels increased with high patient age, low breast density, low BPE, high nuclear grade for DCIS, and increasing tumor size.

Conclusion This study showed that surrounding parenchymal findings and high-risk lesions adjacent to the tumor are not only a stimulus for malignant development, but also a biological factor that directly affects the accuracy of tumor size measurement in imaging modalities. The fact that MRI preserves the highest level of correlation with pathology, even in the presence of complex parenchymal structures and high-risk lesions, justifies its consideration as the primary modality in surgical planning.

Keywords Breast cancer · Tumor size · Surrounding parenchyma · Proliferative changes with atypia · High-risk lesions

Introduction

Tumor size is considered an independent determinant of prognosis, especially in breast cancer patients without axillary lymph node metastasis [1]. Accurate evaluation of this parameter is critical not only in terms of staging but also in treatment planning [1]. In particular, in planning breast-conserving surgical methods such as lumpectomy or quadrantectomy, the tumor size at diagnosis and the ratio of tumor to breast size play a decisive role. In addition to tumor size, the presence of tumor multiplicity such as multifocality, multicentricity and bilaterality also play a key role in selecting the appropriate surgical procedure [2]. Correct determination of these features can positively affect long-term prognosis by reducing the risk of local recurrence [3–6]. In addition, tumor size stands out as an important parameter for the decision of neoadjuvant chemotherapy (NAC) [7–10]. The reduction in tumor size observed after NAC or endocrine therapy is an indicator of response to treatment and

Extended author information available on the last page of the article

also has a prognostic value in terms of overall survival [2, 11]. Therefore, the accuracy of tumor size measurement by clinical examination or imaging methods is of great importance in terms of ensuring the reliability of staging and consistency of the treatment strategy.

Imaging methods such as mammography (MMG), ultrasonography (US), and magnetic resonance imaging (MRI) are widely used in the preoperative assessment of tumor size. The accuracy of the measurements obtained by these methods has been frequently questioned in literature [12–16]. Although radiological findings (such as mammographic breast density, background parenchymal enhancement on MRI, presence of peritumoral edema, tumor localization, etc.), biological (molecular subtype), and histopathological features (histological tumor types of invasive carcinoma, presence of invasive or in situ carcinoma, presence of fibrosis/scar) have been shown to affect tumor size measurement in different modalities, it is still unclear whether surrounding parenchymal features (SPF) affect the accuracy of these measurements [12, 17–20]. The surrounding parenchyma of the primary tumor may show different enhancement patterns on MRI based on differences in age, menopausal status and hormonal changes, which ultimately affect accuracy [21, 22]. Furthermore, benign or high-risk lesions with or without atypia may present as calcifications on mammography as well as mass or non-mass lesions on US and MRI [23]. These lesions may imitate malignancy or create challenges in determining lesion borders, thus leading to mistakes on the assessment of tumor size [24, 25]. The purpose of this study is to evaluate the effect of various radiological, clinical and histological findings in the assessment of tumor size with different radiological modalities, with a particular focus on the effect of surrounding parenchymal features.

Materials and methods

Patient selection

This study is an extension of a previous retrospective multicenter study that evaluated the correlation of tumor sizes measured on different imaging modalities with histopathological tumor sizes according to molecular subtypes and the presence of accompanying ductal carcinoma in situ (DCIS) [12]. In the present analysis, a subgroup of the patients included in the original study, whose SPF were detailed in their pathology reports, is presented.

Eleven university hospitals participated in the study (Turkish Breast Radiology Collaborative TR-BRC 2023-01). Ethics committee approval was obtained for the study (Acibadem University, 2021-21/39). Clinical, radiological and pathological data were entered into a common database (Verifast, Veritas, Clinical Research, 2024 © Copyright VeritasCRO). Patients who were diagnosed with breast cancer between 2010 and 2023, and who had undergone MMG, US, and MRI before primary surgery, were included in the study. Patients who received NAC preoperatively, whose radiological images or postoperative pathology results were unavailable, and who had positive margins at surgical pathology were not included in the database. Patients with more than 1 month interval between imaging and surgery were also excluded in the original study, which comprised of 559 cases finally.

For the present study, pathology reports of these patients were re-evaluated in order to determine if the findings in the surrounding parenchyma were reported. Those patients (n:86) whose pathology reports did not mention any information on the presence or absence of SPFs were excluded from this analysis (Fig. 1), leaving 473 patients for analysis.

As this was a retrospective study based on imaging data collected from institutional archives, there were some patients who were entered in the database although they did not undergo all three (MMG, US and MRI) examinations, but had only two examinations available. These patients were still included in the overall study population ($n=473$), but they were excluded from the specific subgroup analyses (such as lesion type, mammographic breast density and background parenchymal enhancement (BPE)). There were also a few patients whose MRI images were not of high quality, and they were also not taken into consideration in the MRI group. Therefore, MMG, US and MRI findings were evaluated for 462, 473, 436 patients, respectively.

Image analysis

Preoperative MMG, US, and MRI images were accessed via PACS systems and retrospectively reviewed by a single radiologist with at least 5 years of experience in breast imaging at each center based on the 5th version of BI-RADS (Breast Imaging Reporting and Data System) [26]. For each modality, lesion size (largest diameter in mm), lesion type (mass/non-mass/mass + non-mass), mammographic breast density (type A, B, C, D) and background parenchymal enhancement (BPE) on MRI (minimal, mild, moderate, marked) were determined, blinded to the histopathological findings and reports. Calcifications, architectural distortions and asymmetries on mammography were classified as non-mass lesions. In the presence of more than one lesion in the same breast, the largest lesion and its radiological features were included in the study. For statistical analysis, some features were dichotomized as follows: mammographic breast density as fatty (type A or B) or dense (type C or D), BPE on MRI as low (minimal or mild) or intense (moderate or marked).

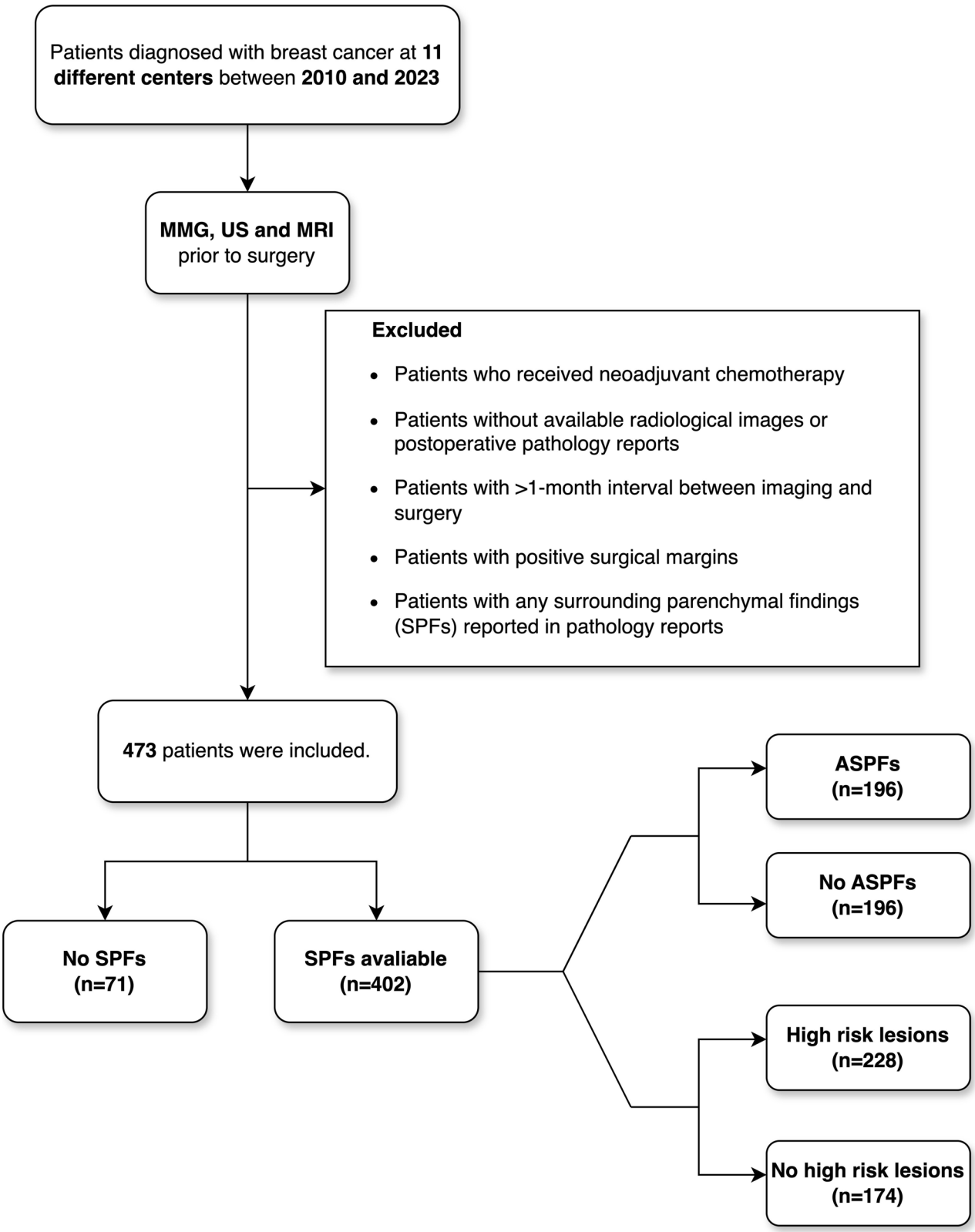

Fig. 1 Flowchart summarizing patient inclusion and exclusion criteria and study flow

Histopathological analysis

The histopathological tumor size in the postoperative pathology report was accepted as the gold standard. Histopathological tumor types were evaluated in three categories: isolated invasive carcinoma, isolated DCIS, and invasive carcinoma accompanied by DCIS (mixed tumor). In mixed tumors, the size of the largest lesion detected on imaging was compared with the total size of the invasive and in situ cancers reported on the pathology report.

Histological tumor types of invasive carcinomas were divided into three categories as invasive ductal carcinoma (IDC), invasive lobular carcinoma (ILC), and others. Based on molecular subtypes, tumors were classified into four groups, Luminal A, Luminal B, HER2-positive, and triple-negative, according to hormone receptor status, HER2 expression, and Ki-67 proliferation index [12]. Histological grading of invasive carcinomas was performed according to the Nottingham histological grading system (Elston–Ellis modification of the Scarff–Bloom–Richardson system), which evaluates tubule formation, nuclear pleomorphism, and mitotic count. Grades 1 and 2 were grouped as low grade, while grade 3 was defined as high grade [27]. For ductal carcinoma in situ (DCIS), nuclear grade was used. Low and intermediate nuclear grades were classified as low grade, and high nuclear grade was defined as high grade [28]. The Van Nuys classification was not applied in this study.

Tumor sizes were evaluated in three groups (0–1 cm, 1–2 cm, >2 cm). This stratification was chosen for both clinical and statistical reasons. The number of patients within the conventional T1 subgroups, especially T1a and T1b, was limited, which restricted the ability to conduct reliable subgroup analyses with adequate statistical power. Therefore, we merged T1a and T1b into a single group (<1 cm), a strategy that has been employed where the sample size or event rate necessitated broader groupings. Tumors <1 cm, particularly in node-negative patients, generally carry an excellent prognosis and may not require aggressive treatment. Conversely, tumors >2 cm are often considered for neoadjuvant chemotherapy or more extensive surgical approaches [29]. Considering this clinical approach, a modified T stage classification was made.

Histopathological evaluations were performed by a single experienced pathologist in each center.

Categorization of SPFs

SPFs were categorized into three groups as those with no findings (as stated in the pathology report), those with benign lesions (such as fibrocystic changes, fibroadenoma, proliferative lesions without atypia), and those with high-risk lesions. SPFs were further subdivided as those with or without atypia. Radial scar, papillary lesions, and phyllodes tumor were categorized as high-risk lesions without atypia, while atypical ductal hyperplasia (ADH), atypical lobular hyperplasia (ALH), lobular carcinoma in situ (LCIS), and flat epithelial atypia (FEA) were considered lesions with atypia (ASPF) [30].

Correlation coefficients (r) and significance levels (p) were compared according to the presence of any SPFs, SPFs in the form of high-risk lesions and atypical SPFs (ASPF). Furthermore, effects of patient age, physical findings (palpable, non-palpable), histopathological findings and radiological features on the accuracy of size measurement by MMG; US and MRI were evaluated. For statistical analysis, patient age was divided into two categories as ≥50 and <50. The reason for this categorization was that age 50 is considered generally as the age of menopause, and after this age, the effect of hormonal changes on the breast should decrease [31]. (As this study is retrospective, it was not possible to collect data on the menopausal status of patients.)

Statistical analysis

Patient data collected within the scope of the study were analyzed using the IBM Statistical Package for the Social Sciences (SPSS) for Mac OS 30.0 (IBM Corp., Armonk, NY) package program. A two-tailed Kolmogorov–Smirnov test was applied to examine for whether the continuous quantitative variables follow a Gaussian distribution. Frequency and percentage were given for categorical data, mean, standard deviation (SD), median and interquartile range descriptive values for continuous data. "Spearman Correlation Analysis" was used for examining the relationship between continuous variables. The results were considered statistically significant when the p-value was less than 0.05.

If the correlation coefficient is positive as a result of the significant relationship between the variables, it indicates that there is a positive linear relationship between the variables, and if it is negative, it indicates that there is a negative linear relationship. The value ranges of the correlation coefficient are expressed as follows: Correlation coefficient: a relationship between 0.00 and 0.29 indicates a weak; between 0.30 and 0.49 indicates a low; between 0.50 and 0.69 indicates a moderate; between 0.70 and 0.89 indicates a strong; between 0.90 and 1.00 indicates a very strong relationship between the two variables [32]. To enhance statistical transparency, all correlation coefficients reported in this study were accompanied by 95% confidence intervals. This allows the reader to evaluate the uncertainty around each estimate and interpret subgroup analyses with appropriate caution.

Results

A total of 473 patients were included in the study. The mean age of the patients was 51 ± 11 years (26–91), and 48.8% (*n*:231) were younger than age 50. While 67.2% (*n*:318) of lesions were invasive, 25.6% (*n*:121) were mixed, and 7.2% (*n*:34) were pure DCIS. The mean histopathological size was 20.2 ± 23.7 mm for DCIS cases, 37.8 ± 28.5 mm for mixed tumors and 22.0 ± 16.2 mm for invasive cancers. While 39.4% (*n*:61) of DCIS were low grade and 60.6% (*n*:94) were high grade, 64.9% (*n*:285) of invasive tumors were low grade and 35.1% (*n*:154) were high grade.

Of all invasive tumors, 80.2% were IDC and 12.1% were ILC. 20% of invasive tumors were smaller than 1 cm, 40.1% were 1–2 cm, and 39.9% were >2 cm. There were concomitant SPFs in 402 patients (85%), and 228 of these patients (56.7%) had high-risk lesions, of which 196 (48.8%) were ASPFs (Table 1).

The correlation of radiological and pathological size measurements based on the presence or absence of any SPFs are presented in Table 2. For invasive cancers, correlation was better for MMG and US (*r*:0.666 vs *r*:0.450 and *r*:0.769 vs *r*:0.670, respectively) when there were no SPFs, however MRI measurements showed moderate correlation in all cases. For DCIS cases, correlation was again better for MMG (*r*:0.555 vs *r*:0.334) when there were no SPFs, and again there was no difference on the accuracy of MRI measurements (*r*: 0.546 vs 0.509). However, US measurements correlated significantly with pathology only when SPFs were present, whereas no significant correlation was observed when SPFs were absent (*r*:0.208 vs 0.306). For mixed tumors, surprisingly, both US (*r*: 0.720 vs *r*:0.309) and MRI (*r*:0.791 vs *r*:0.487) measurements correlated better when there were SPFs, while there was no difference for MMG (Figs. 2, 3).

The correlation of sizes based on the presence or absence of atypical high-risk lesions in the surrounding parenchyma are presented in Table 3. In DCIS cases, the size measurements of MMG and MRI did not show a significant correlation with pathological sizes in cases with atypical proliferative lesions in the surrounding parenchyma, while MRI measurements showed moderate correlation if ASPFs were not present. Presence or absence of ASPFs did not affect the level of agreement of radiological measurements in mixed tumors, although the MRI measurements showed some increase in accuracy when atypical lesions were absent (*r*:0.847 vs *r*:0.718). Interestingly, level of agreement increased from moderate to strong for both US (*r*:0.753 vs *r*:0.582) and MRI (*r*:0.770 vs *r*:0.568) in invasive cases in the presence of ASPFs, while MMG measurements showed weak agreement in all cases.

Correlation between radiological and pathological measurements based on the presence of any high-risk lesions in the surrounding parenchyma are presented in Table 4. The agreement levels did not change for any modality in invasive and mixed cancers, although accuracy of MRI increased slightly if there were no high risk lesions in cases with mixed tumors (*r*:0.838 vs *r*:0.748). Correlation was worse for all modalities when these lesions were present in the surrounding parenchyma in DCIS cases (MMG *r*: 0.461 vs 0.291, US *r*: 0.306 vs 0.269, MRI *r*:0.683 vs 0.313), and there was not even a significant relationship with pathology for MMG and US in that scenario ($p > 0.05$).

When the effects of other factors on the accuracy of size measurements were evaluated (Suppl. Tables 1–10), it was seen that the agreement levels of MRI measurements increased in all tumor types in patients older than age 50, compared to younger patients, although the increase was minimal in invasive cancers. MMG and US accuracy also increased in older patients in invasive and mixed tumors. In DCIS, age did not affect accuracy of measurements in US, while it was better in young patients at MMG (Suppl. Table 1). The correlation levels were higher in fatty breasts for all modalities in invasive and mixed tumors, but it affected only MMG for DCIS cases (Suppl. Table 2). Intense BPE caused a decrease in the accuracy of measurements of all tumors on MRI; but the decrease was minimal for invasive cancers. BPE caused a major difference in measurements of only invasive tumors on MMG and US (Suppl. Table 3). In terms of tumor grade, measurements were more accurate in mixed tumors with all modalities if the DCIS component was high grade, and with MMG and MRI in pure DCIS cases (Suppl. Table 4). On the other hand tumor grade of invasive cancers did not affect accuracy of measurements (Suppl. Table 5). For lobular cancers, MRI demonstrated a numerically stronger correlation with pathological size (Suppl. Table 6). While MMG and US showed moderate levels of agreement, overlapping confidence intervals prevent formal conclusions about modality superiority. When evaluated according to molecular subtypes, MRI demonstrated numerically higher correlation coefficients with histopathological tumor size across all groups. The strongest correlation was observed in mixed tumors with Luminal B subtype (*r*:0.853, 95% CI: 0.678–0.936), although overlapping confidence intervals between subtypes and modalities indicate that these differences should be interpreted with caution (Suppl. Table 7). Lesion type and physical examination findings did not have any effect on the accuracy of size measurements (Suppl. Tables 8–9). In terms of lesion size, lowest agreement was with invasive cancers that were smaller than 1 cm in all modalities, and the highest correlation was achieved with MRI in larger tumors (Suppl. Table 10).

Table 1. General characteristics of patients and tumors included in the study

Variables ($n=473$)	n (%)	Mean ± SD	Median (IQR)
Age		51 ± 11	50 (43–58)
<50	231 (48.8)		
≥50	242 (51.2)		
Mammographic breast density			
Fatty (Type A + B)	164 (35.5)		
Dense (Type C + D)	298 (64.5)		
BPE			
Low (Minimal + Mild)	277 (63.5)		
Intense (Moderate + Marked)	159 (36.5)		
Type of the tumor			
DCIS	34 (7.2)		
Mixed tumor (DCIS + Invasive)	121 (25.6)		
Invasive	318 (67.2)		
DCIS grade	***n* = 155**		
Low (grade I–II)	61 (39.4)		
High (grade III)	94 (60.6)		
Invasive tumor grade	***n* = 439**		
Low (grade I–II)	285 (64.9)		
High (grade III)	154 (35.1)		
Tumor size (mm)			
DCIS		20.2 ± 23.7	10 (4–25)
Mixed tumors		37.8 ± 28.5	30 (22–45.5)
Invasive tumors		22.0 ± 16.2	18 (12–25)
<10 mm	88 (20.0)		
10–20 mm	176 (40.1)		
≥20 mm	175 (39.9)		
Histological type of invasive tumor (mm)	***n* = 439**		
Invasive ductal	352 (80.2)	18.6 ± 15.8	18 (12–25)
Invasive lobular	53 (12.1)	24.2 ± 27	22 (15–35)
Other	34 (7.7)	19.2 ± 18.45	21 (13–32)
Molecular subtype of invasive tumor (mm)*			
Luminal A	219 (46.3)	21.2 ± 16.9	18 (12–25)
Luminal B	111 (23.5)	20.6 ± 12.6	18.5 (12–25)
HER2-positive	77 (16.3)	26.3 ± 15.7	22.5 (13–30)
Triple-negative	66 (14.0)	25.8 ± 14.9	20(15–27)
SPF ($n=473$)			
Present	402 (85)		
Absent	71 (15)		
ASPF ($n=402$)			
Present	196 (48.8)		
Absent	206 (51.2)		
High-risk lesion ($n=402$)			
Present	228 (56.7)		
Absent	174 (43.3)		

Bold values indicate statistically significant results ($p < 0.05$)

*Categorized as: (Ki-67>14%)

IQR Interquartile range, *SPF* Surrounding parenchymal findings, *ASPF* Atypical surrounding parenchymal findings, *BPE* Background parenchymal enhancement, *DCIS* Ductal carcinoma in situ, *HER2* Human epidermal growth factor receptor 2

Table 2. Evaluation of the agreement between histopathological tumor sizes and radiological sizes according to the presence of surrounding parenchymal findings

Size	Surrounding parenchymal findings		Mixed tumor size	DCIS size	Invasive tumor size
Tumor size on MMG	Present	*r* (95% CI)	**0.511 (0.338–0.651)**	**0.334 (0.157–0.490)**	**0.450 (0.356–0.535)**
		p-value	**<0.001**	**<0.001**	**<0.001**
	Absent	*r* (95% CI)	**0.504 (0.033–0.791)**	**0.555 (0.183–0.788)**	**0.666 (0.483–0.793)**
		p-value	**0.033**	**0.005**	**<0.001**
Tumor size on US	Present	*r* (95% CI)	**0.720 (0.596–0.810)**	**0.306 (0.116–0.473)**	**0.670 (0.606–0.726)**
		p-value	**<0.001**	**0.001**	**<0.001**
	Absent	*r* (95% CI)	0.309 (−0.183–0.677)	0.208 (−0.247–0.587)	**0.769 (0.638–0.856)**
		p-value	0.198	0.354	**<0.001**
Tumor size on MRI	Present	*r* (95% CI)	**0.791 (0.697–0.858)**	**0.509 (0.356–0.635)**	**0.668 (0.604–0.723)**
		p-value	**<0.001**	**<0.001**	**<0.001**
	Absent	*r* (95% CI)	**0.487 (0.057–0.765)**	**0.546 (0.190–0.775)**	**0.582 (0.382–0.729)**
		p-value	**0.025**	**0.004**	**<0.001**

Bold values indicate statistically significant results ($p < 0.05$)

MMG Mammography, *US* Ultrasonography, *MRI* Magnetic resonance imaging, *DCIS* Ductal carcinoma in situ, *r*Correlation coefficient, *CI* Confidence interval

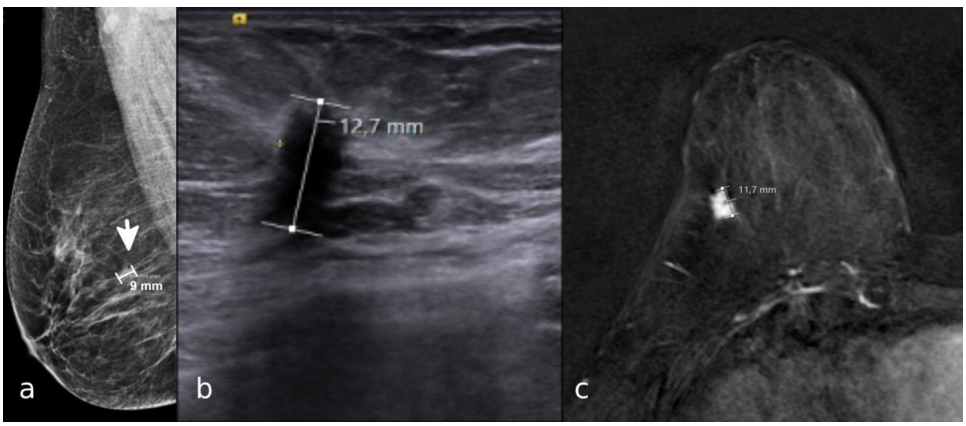

Fig. 2 A 55-year-old female patient with a non-palpable tumor in the lower outer quadrant of her right breast had a lesion size of 9 mm on MMG (**a**), 12.7 mm on US (**b**), and 11.7 mm on MRI (**c**). The pathology result was invasive ductal carcinoma (invasive ductal carcinoma (IDC), NOS, grade II, ER = %90, PR = %55, Ki-67:7%) and the tumor diameter was reported as 13 mm. The tumor sizes measured by US and MRI were similar to the pathological sizes of the tumor. There were no surrounding parenchymal findings in the pathology report

Discussion

This study is an extension of a previous retrospective multicenter study we have published; where we had compared the accuracy of size measurement of breast cancers with MMG, US and MRI, based on different molecular subtypes and presence of accompanying DCIS [12]. In that former study, we had shown that MRI is the most reliable method for determining preoperative tumor size of invasive and in-situ tumors and all molecular subtypes, although accuracy dropped in cases with pure or mixed DCIS. In this subgroup analysis, we aimed to determine the effects of various clinical, radiological and pathological findings on the accuracy of lesion sizes measured on different radiological modalities. Our primary focus was to

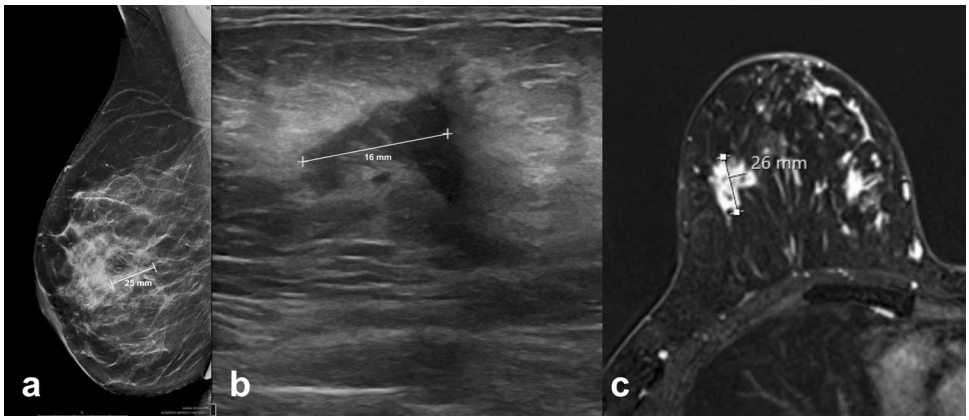

Fig. 3 A 39-year-old woman with a palpable tumor in the upper outer quadrant of her right breast showed pathological microcalcifications and accompanying distortion in an area of approximately 25 mm on MMG (**a**). The widest lesion size measured 16 mm on US (**b**) and 26 mm on axial contrast-enhanced fat-suppressed T1-weighted MRI images (**c**). Postoperative pathology revealed in situ + invasive carcinoma, with an in situ (high-grade) size of 10 mm and an invasive size of 25 mm (invasive ductal carcinoma (IDC), NOS, grade II, ER: 80%, PR: 10%, Ki-67:20%) with surrounding atypical hyperplastic changes

Table 3. Evaluation of the agreement between histopathological tumor sizes and radiological sizes according to the presence of atypical surrounding parenchymal findings

Size	Atypical surrounding parenchymal findings		Mixed tumor size	DCIS size	Invasive tumor size
Tumor size on MMG	Present	*r* (95% CI)	**0.525 (0.258–0.717)**	0.193 (−0.112–0.465)	**0.493 (0.362–0.604)**
		p-value	**<0.001**	0.199	**<0.001**
	Absent	*r* (95% CI)	**0.515 (0.268–0.698)**	**0.485 (0.278–0.650)**	**0.406 (0.266–0.529)**
		p-value	**<0.001**	**<0.001**	**<0.001**
Tumor size on US	Present	*r* (95% CI)	**0.719 (0.521–0.843)**	**0.335 (0.033–0.581)**	**0.753 (0.679–0.812)**
		p-value	**<0.001**	**0.026**	**<0.001**
	Absent	*r* (95% CI)	**0.715 (0.529–0.835)**	**0.320 (0.069–0.533)**	**0.582 (0.470–0.676)**
		p-value	**<0.001**	**0.011**	**<0.001**
Tumor size on MRI	Present	*r* (95% CI)	**0.718 (0.531–0.838)**	0.220 (−0.080–0.484)	**0.770 (0.701–0.824)**
		p-value	**<0.001**	0.137	**<0.001**
	Absent	*r* (95% CI)	**0.847 (0.738–0.913)**	**0.679 (0.523–0.791)**	**0.568 (0.454–0.663)**
		p-value	**<0.001**	**<0.001**	**<0.001**

Bold values indicate statistically significant results ($p < 0.05$)

MMG Mammography, *US* Ultrasonography, *MRI*: Magnetic resonance imaging, *DCIS* Ductal carcinoma in situ, *r* Correlation coefficient, *CI* Confidence interval

evaluate the effects of SPFs with or without atypia. To the best of our knowledge, this is the first study that evaluates the effects of findings in the surrounding parenchyma on the accuracy of radiological tumor size measurements in breast cancer.

There were concomitant SPFs in 85% (*n*:402) of our patients. More than half (228/402) of these lesions were high-risk lesions, most of which (196/228) were lesions with atypia. These ratios are very high and support previous studies reporting that SPFs in the form of high-risk lesions with or without atypia are more common in breast cancer patients compared to the normal population [33, 34]. Hoogerbrugge et al. have also reported that high risk lesions are detected in 71% of BRCA mutation carriers, but

Table 4. Evaluation of the agreement between histopathological tumor sizes and radiological sizes according to the presence of high-risk lesions

Size	High-risk lesions		Mixed tumor size	DCIS size	Invasive tumor size
Tumor size on MMG	Present	*r* (95% CI)	**0.526 (0.288–0.703)**	**0.291 (0.033–0.513)**	**0.411 (0.281–0.527)**
		p-value	**<0.001**	**0.024**	**<0.001**
	Absent	*r* (95% CI)	**0.525 (0.250–0.721)**	**0.461 (0.220–0.649)**	**0.487 (0.344–0.607)**
		p-value	**<0.001**	**<0.001**	**<0.001**
Tumor size on US	Present	*r* (95% CI)	**0.739 (0.575–0.846)**	**0.269 (0.001–0.501)**	**0.684 (0.601–0.753)**
		p-value	**<0.001**	**0.043**	**<0.001**
	Absent	*r* (95% CI)	**0.701 (0.480–0.838)**	**0.306 (0.019–0.547)**	**0.651 (0.543–0.737)**
		p-value	**<0.001**	**0.032**	**<0.001**
Tumor size on MRI	Present	*r* (95% CI)	**0.748 (0.596–0.849)**	**0.313 (0.057–0.531)**	**0.683 (0.601–0.751)**
		p-value	**<0.001**	**0.015**	**<0.001**
	Absent	*r* (95% CI)	**0.838 (0.706–0.914)**	**0.683 (0.509–0.804)**	**0.647 (0.539–0.734)**
		p-value	**<0.001**	**<0.001**	**<0.001**

MMG: Mammography, *US* Ultrasonography, *MRI* Magnetic resonance imaging, *DCIS* Ductal carcinoma in situ, *r* Correlation coefficient, *CI* Confidence interval

in only 43% of non-carriers [35]. These lesions are clues of a biologically more active background parenchyma in breast cancer patients, and support the need of active surveillance in patients with high-risk lesions detected on percutaneous biopsies. Considering that MRI is the method with highest sensitivity and accuracy in breast cancer detection, it could be a very good alternative to conventional methods in the screening of these patients, especially for those with dense breasts. This is also supported by a recent study reported by Salim et al. where the cancer detection rate with MRI in patients with a complex parenchyma as determined by machine learning methods was very high (64/1000), much higher than in patients that are actually categorized as high-risk patients [36].

High-risk lesions in the parenchyma are important not only as a sign of increased risk, but also as a factor that affects accuracy of lesion size assessment on imaging [30]. They imitate findings of malignancy, thus making the determination of lesion boundaries difficult. Our results showed that the presence of high-risk lesions, especially those with atypia, was most effective on the MRI measurement of pure DCIS cases. The correlation level of MRI measurements dropped to 0.313 from 0.683 when high-risk lesions were present, and the difference was even higher (0.220 vs 0.679) in the presence of atypical proliferative lesions. The same effect was observed also in the MMG measurements of DCIS cases. However, even when these lesions were not present, its accuracy was lower compared to MRI. High-risk lesions usually present as non-mass lesions on MMG and MRI, similar to DCIS. Therefore, they can be expected to cause a negative effect on the accuracy of measurement in cases of DCIS, as seen in our findings. On the other hand, our results show that the US measurements are not affected by the presence of these lesions, probably because some of them do not present as a measurable finding on US, and even DCIS itself cannot be detected in an important percentage of patients. In cases with mixed tumors, the accuracy of MRI measurements decreased but those of MMG and US did not change. The drop in MRI was lower compared to cases with pure DCIS, not leading to a change in the level of correlation.

Surprisingly, presence of atypical proliferative lesions in the surrounding parenchyma increased the accuracy of size measurement of invasive cancers on US and MRI, while there was no difference on MMG. Invasive cancers usually present as mass lesions. When the correlation of radiological and pathological lesion sizes was evaluated based on lesion type in our study, it was found that correlation was better in mass lesions compared to non-mass lesions in invasive cancers. This may be a reason for this discrepency, however these results need to be verified in prospective larger studies with a higher number of cases in each subgroup.

When the effect of any SPF was evaluated, we showed that even benign proliferative lesions affected the accuracy of MMG. Level of correlation dropped to 0.334 from 0.555 in DCIS, and to 0.450 from 0.666 in invasive cancers. Although a similar effect was observed on US for invasive tumors, the increase in diagnostic performance compared

to non-invasive tumors was limited (*r*: 0.670 vs 0.769), suggesting a less pronounced improvement. Again unexpectedly, size measurements were more accurate for mixed tumors on US and MRI in the presence of SPFs. A potential explanation for this finding may be that both methods actually underestimate lesion size, and in the presence of other lesions nearby, the lesions appear larger, leading to a more accurate determination of lesion size. Another possibility for MRI is that breasts with many proliferative lesions are more bioactive and the vascularity is increased, thus leading to more accurate representation of the tumoral lesions on images. As previously stated, this paper is the first in literature evaluating the effect of SPFs with and without atypia on the accuracy of radiological measurement of breast cancer, and the results need to be verified in larger studies.

When other factors were evaluated, all measurements were more accurate on MRI in patients older than age 50, and in patients with low BPE. This is an expected finding, since menstrual changes are less affective in this age group. This aligns with prior studies showing that menstrual hormonal fluctuations elevate BPE, which can obscure lesion boundaries and decrease measurement accuracy; conversely, less hormonally active breasts yield clearer delineation and better MRI-pathology correlation [37]. Similarly, it was noted that in patients with intense BPE, US and MMG accuracy, as well as MRI compatibility, generally decreased, which is consistent with the literature [25, 38]. On the other hand, age did not affect measurement on US and MMG for DCIS. Lesion measurements were more accurate in fatty breasts for all modalities in all types of tumors, with the exception of DCIS on MMG, which was not affected by density. This is also an expected finding, since BPE is also decreased in these patients and fatty breasts are more common in older patients. It has also been suggested that the relative low incidence of SPFs in fatty breasts may be a contributing factor [39, 40]. The US RSNA review similarly reports that dense fibroglandular tissue impairs both lesion detection and size-estimation, resulting in greater discordance compared to fatty breasts [41]. Consistent with literature, the measurements of invasive tumors that presented as a mass lesion was more accurate in all modalities, but lesion type did not affect measurement in other types of cancers [15].

Tumor grade was affective in DCIS cases but not in invasive cancers. Measurement was more accurate in pure and mixed DCIS cases in all modalities if the DCIS component was high grade in accordance with the literature [42, 43]. When we look at tumor type, our results showed that the measurement of cancers other than IDC and ILC were more accurate on all modalities, probably because these lesions usually present as mass lesions with definite margins. For lobular carcinomas, MRI demonstrated numerically higher correlation coefficients with pathological size compared to other modalities, supporting the findings of previous studies on this subject [44]. Another interesting finding of our study was that the lowest correlation coefficients were observed in invasive cancers smaller than 1 cm across all imaging modalities. MRI showed numerically higher correlation values for tumors of all sizes, though overlapping confidence intervals suggest these differences should be interpreted with caution and not considered statistically significant.

Limitations

One of the limitations of our study is the relatively small number of patients. The unbalanced distributions in subgroups may have affected the results of the study. The relatively low number of patients in some subgroups may have led to limitations in terms of statistical significance and generalizability. Furthermore, the retrospective and multicenter nature of the study make standardization difficult. Pathologists in different centers may have different priorities in reporting SPFs, however due to the high number of patients with SPFs, we think that all pathologists gave detailed information about the surrounding parenchymal findings. Similarly, MRI, MMG and US images were obtained at different centers with different devices and protocols, and evaluated by a different radiologist at each center. This may have caused interobserver variation. However, this was actually the reason this study was designed as a multicenter study, in order to prevent observer bias, and all the measurements were made by dedicated breast radiologists with at least 5 years of experience. Another limitation is the potential discrepancy in tumor size measurements due to differences in the orientation of imaging planes and pathological slicing. Since radiological assessments, especially in MG and US, are obtained in standardized yet limited planes, they may not always align with the pathological long axis, potentially affecting the accuracy of size correlation. Although the time interval between imaging and surgery was less than 1 month, some aggressive tumors may have grown rapidly during that time. Tissue shrinkage and changes in sampling methods at pathology can also lead to underestimation of tumor size. In addition, the large amount of tissue taken in preoperative biopsies, especially vacuum biopsy, may have caused differences in radiological and pathological measurements.

Conclusion

This study showed that surrounding parenchymal findings and high-risk lesions adjacent to the tumor are not only a stimulus for malignant development, but also a biological factor that directly affects the accuracy of tumor size measurement in imaging modalities. The fact that MRI preserves

the higher level of pathological measurement accuracy even in the presence of complex parenchymal structures and high-risk lesions, justifies its consideration as the primary modality in surgical planning. On the other hand, the frequent presence of high-risk lesions in the breast parenchyma indicates that these women require more intensive and multidisciplinary follow-up. Appropriate adaptive imaging strategies and personalized screening approaches may both increase diagnostic accuracy and reduce unnecessary invasive procedures for this group of patients.

Supplementary Information The online version contains supplementary material available at https://doi.org/10.1007/s11604-025-01895-2.

References

1. Liu Y, He M, Zuo WJ, Hao S, Wang ZH, Shao ZM. Tumor size still impacts prognosis in breast cancer with extensive nodal involvement. Front Oncol. 2021;11:585613. https://doi.org/10.3389/fonc.2021.585613.
2. Tong Y, Sun F, Zhang C, Yang S, Yu Z, Zhao Y. Multifocal/multicentric breast cancer: does each focus matter? Cancer Med. 2023;12(7):8815–24. https://doi.org/10.1002/cam4.5626.
3. Sun Y, Gao L, Zhou X, Wang Z, Li Y, Sun Q. Local recurrence and survival outcomes of multifocal/multicentric breast cancer after breast conserving therapy: a systematic review and meta-analysis. Clin Breast Cancer. 2025;25(3):e229–e239.e9. https://doi.org/10.1016/j.clbc.2024.10.009. Epub 2024 Oct 18. PMID: 39542811.
4. Chung AP, Huynh K, Kidner T, Mirzadehgan P, Sim MS, Giuliano AE. Comparison of outcomes of breast conserving therapy in multifocal and unifocal invasive breast cancer. J Am Coll Surg. 2012;215(1):137–46; discussion 146–7. https://doi.org/10.1016/j.jamcollsurg.2012.05.006. Epub 2012 May 18. PMID: 22608402.
5. Houvenaeghel G, Tallet A, Jalaguier-Coudray A, Cohen M, Bannier M, Jauffret-Fara C, et al. Is breast conservative surgery a reasonable option in multifocal or multicentric tumors? World J Clin Oncol. 2016;7(2):234–42. https://doi.org/10.5306/wjco.v7.i2.234.PMID:27081646;PMCID:PMC4826969.
6. Gwak H, Jung SH, Suh YJ, Nam SJ, Han JH, Oh SJ, et al. Prognostic impact of multiple synchronous T1 breast cancer. Cancers (Basel). 2024;30(23):4019. https://doi.org/10.3390/cancers16234019.
7. Mougalian SS, Soulos PR, Killelea BK, Lannin DR, Abu-Khalaf MM, DiGiovanna MP, et al. Use of neoadjuvant chemotherapy for patients with stage I to III breast cancer in the United States. Cancer. 2015;121(15):2544–52. https://doi.org/10.1002/cncr.29348.
8. Rubio IT, Sobrido C. Neoadjuvant approach in patients with early breast cancer: patient assessment, staging, and planning. Breast. 2022;62(1):S17–24. https://doi.org/10.1016/j.breast.2021.12.019.
9. Song D, Man X, Jin M, Li Q, Wang H, Du Y. A decision-making supporting prediction method for breast cancer neoadjuvant chemotherapy. Front Oncol. 2021;10:592556. https://doi.org/10.3389/fonc.2020.592556.
10. Lee SY, Yoo TK, Lee SB, Kim J, Chung IY, Ko BS, et al. Prognostic value of residual cancer burden after neoadjuvant chemotherapy in breast cancer: a comprehensive subtype-specific analysis. Sci Rep. 2025;15(1):13977. https://doi.org/10.1038/s41598-025-98176-9.
11. Korde LA, Somerfield MR, Carey LA, Crews JR, Denduluri N, Hwang ES, et al. Neoadjuvant chemotherapy, endocrine therapy, and targeted therapy for breast cancer: ASCO guideline. J Clin Oncol. 2021;39(13):1485–505. https://doi.org/10.1200/JCO.20.03399.
12. Sanli DET, Icten GE, Kul S, Balci P, Tuncbilek N, Celik L, Kayadibi Y, Oktay A, Gultekin S, Taskin F, Aribal ME, Ozveri E, Tokat F, Teymur A, Akin IB, Ozdemir G, Guner DC, Kurt SA, Aslan O, Aslan AA, Yilmaz E. Correlation of radiological and pathological tumor sizes in breast cancer based on molecular subtypes and accompanying DCIS: a retrospective multicenter study. TR-BRC 2023-01. Acad Radiol. 2025; S1076–6332(25)00092–3. https://doi.org/10.1016/j.acra.2025.01.037. Epub ahead of print. PMID: 39984336.
13. Baek SH, Choi WJ, Cha JH, Kim HH, Shin HJ, Chae EY. Comparison of mammography, ultrasound, and MRI in size assessment of ductal carcinoma in situ with histopathologic correlation. Acta Radiol. 2017;58(12):1434–41. https://doi.org/10.1177/0284185117698860.
14. Preibsch H, Beckmann J, Pawlowski J, Kloth C, Hahn M, Staebler A, et al. Accuracy of breast magnetic resonance imaging compared to mammography in the preoperative detection and measurement of pure ductal carcinoma in situ: a retrospective analysis. Acad Radiol. 2019;26(6):760–5. https://doi.org/10.1016/j.acra.2018.07.013.
15. Azhdeh S, Kaviani A, Sadighi N, Rahmani M. Accurate estimation of breast tumor size: a comparison between ultrasonography, mammography, magnetic resonance imaging, and associated contributing factors. Eur J Breast Health. 2020;17(1):53–61. https://doi.org/10.4274/ejbh.2020.5888.PMID:33796831;PMCID:PMC8006785.
16. Cortadellas T, Argacha P, Acosta J, Rabasa J, Peiró R, Gomez M, et al. Estimation of tumor size in breast cancer comparing clinical examination, mammography, ultrasound and MRI-correlation with the pathological analysis of the surgical specimen. Gland Surg. 2017;6(4):330–5. https://doi.org/10.21037/gs.2017.03.09.
17. Mennella S, Garlaschi A, Paparo F, Perillo M, Celenza M, Massa T, et al. Magnetic resonance imaging of breast cancer: factors affecting the accuracy of preoperative lesion sizing. Acta Radiol. 2015;56(3):260–8. https://doi.org/10.1177/0284185114524089.
18. Yoo EY, Nam SY, Choi HY, Hong MJ. Agreement between MRI and pathologic analyses for determination of tumor size and correlation with immunohistochemical factors of invasive breast carcinoma. Acta Radiol. 2018;59(1):50–7. https://doi.org/10.1177/0284185117705010.
19. Hamza A, Khawar S, Sakhi R, Alrajjal A, Miller S, Ibrar W, et al. Factors affecting the concordance of radiologic and pathologic tumor size in breast carcinoma. Ultrasound. 2019;27(1):45–54. https://doi.org/10.1177/1742271X18804278.
20. Abu Abeelh E, AbuAbeileh Z. Comparative effectiveness of mammography, ultrasound, and MRI in the detection of breast carcinoma in dense breast tissue: a systematic review. Cureus. 2024;16(4):e59054. https://doi.org/10.7759/cureus.59054.
21. Karimi Z, Phillips J, Slanetz P, Lotfi P, Dialani V, Karimova J, et al. Factors associated with background parenchymal enhancement on contrast-enhanced mammography. AJR Am J Roentgenol. 2021;216(2):340–8. https://doi.org/10.2214/AJR.19.22353.
22. Nissan N, Bauer E, Moss Massasa EE, Sklair-Levy M. Breast MRI during pregnancy and lactation: clinical challenges and technical advances. Insights Imaging. 2022;13(1):71. https://doi.org/10.1186/s13244-022-01214-7.
23. Heller SL, Moy L. Imaging features and management of high-risk lesions on contrast-enhanced dynamic breast MRI. AJR Am J Roentgenol. 2012;198(2):249–55. https://doi.org/10.2214/AJR.11.7610.
24. Kim SY, Lee HS, Kim EK, Kim MJ, Moon HJ, Yoon JH. Effect of background parenchymal enhancement on pre-operative breast magnetic resonance imaging: how it affects interpretation and the

role of second-look ultrasound in patient management. Ultrasound Med Biol. 2016;42(12):2766–74. https://doi.org/10.1016/j.ultrasmedbio.2016.08.008.
25. Baek JE, Kim SH, Lee AW. Background parenchymal enhancement in breast MRIs of breast cancer patients: impact on tumor size estimation. Eur J Radiol. 2014;83:1356–62 ((**PMID: 24882786**)).
26. D'Orsi CJ, Sickles EA, Mendelson EB, Morris EA. ACR BI-RADS® Atlas, Breast Imaging Reporting and Data System. 5th ed. Reston, VA: American College of Radiology; 2013.
27. Elston CW, Ellis IO. Pathological prognostic factors in breast cancer. I. The value of histological grade in breast cancer: experience from a large study with long-term follow-up. Histopathology. 1991;19(5):403–10.
28. Schuh F, Biazús JV, Resetkova E, Benfica CZ, Ventura Ade F, Uchoa D, et al. Histopathological grading of breast ductal carcinoma in situ: validation of a web-based survey through intra-observer reproducibility analysis. Diagn Pathol. 2015;10(10):93. https://doi.org/10.1186/s13000-015-0320-2.PMID:26159429;PMCID:PMC4702358.
29. Giuliano AE, Connolly JL, Edge SB, Mittendorf EA, Rugo HS, Solin LJ, et al. Breast cancer-major changes in the American Joint Committee on Cancer eighth edition cancer staging manual. CA Cancer J Clin. 2017;67(4):290–303. https://doi.org/10.3322/caac.21393.
30. Catanzariti F, Avendano D, Cicero G, Garza-Montemayor M, Sofia C, Venanzi Rullo E, et al. High-risk lesions of the breast: concurrent diagnostic tools and management recommendations. Insights Imaging. 2021;12(1):63. https://doi.org/10.1186/s13244-021-01005-6.
31. Appiah D, Nwabuo CC, Ebong IA, Wellons MF, Winters SJ. Trends in age at natural menopause and reproductive life span among US women, 1959–2018. JAMA. 2021;6(13):1328–30. https://doi.org/10.1001/jama.2021.0278.
32. Papageorgiou SN. On correlation coefficients and their interpretation. J Orthod. 2022;49(3):359–61. https://doi.org/10.1177/14653125221076142.
33. Arun B, Vogel KJ, Lopez A, Hernandez M, Atchley D, Broglio KR, et al. High prevalence of preinvasive lesions adjacent to BRCA1/2-associated breast cancers. Cancer Prev Res (Phila). 2009;2(2):122–7. https://doi.org/10.1158/1940-6207.CAPR-08-0050.
34. Harbhajanka A, Gilmore HL, Calhoun BC. High-risk and selected benign breast lesions diagnosed on core needle biopsy: evidence for and against immediate surgical excision. Mod Pathol. 2022;35(11):1500–8. https://doi.org/10.1038/s41379-022-01092-w. (**Epub 2022 Jun 2 PMID: 35654997**).
35. Hoogerbrugge N, Bult P, Bonenkamp JJ, Ligtenberg MJ, Kiemeney LA, de Hullu JA, et al. Numerous high-risk epithelial lesions in familial breast cancer. Eur J Cancer. 2006;42(15):2492–8. https://doi.org/10.1016/j.ejca.2006.05.027.
36. Salim M, Liu Y, Sorkhei M, Ntoula D, Foukakis T, Fredriksson I, et al. AI-based selection of individuals for supplemental MRI in population-based breast cancer screening: the randomized screentrustmri trial. Nat Med. 2024;30(9):2623–30. https://doi.org/10.1038/s41591-024-03093-5.
37. Liao GJ, Henze Bancroft LC, Strigel RM, Chitalia RD, Kontos D, Moy L, et al. Background parenchymal enhancement on breast MRI: a comprehensive review. J Magn Reson Imaging. 2020;51(1):43–61. https://doi.org/10.1002/jmri.26762.
38. Kang SY, Ahn H, Byon J, Youn H, Jung S. Comparative accuracy of preoperative tumor size assessment on ultrasonography and magnetic resonance imaging in ductal carcinoma in situ. J Breast Dis. 2021;9:37–44. https://doi.org/10.14449/jbd.2021.9.2.37.
39. Ghosh K, Vierkant RA, Frank RD, Winham S, Visscher DW, Pankratz VS, et al. Association between mammographic breast density and histologic features of benign breast disease. Breast Cancer Res. 2017;19(1):134. https://doi.org/10.1186/s13058-017-0922-6.
40. Sitges C, Mann RM. Breast MRI to screen women with extremely dense breasts. J Magn Reson Imaging. 2025;62(1):58–72. https://doi.org/10.1002/jmri.29716.
41. Freer PE. Mammographic breast density: impact on breast cancer risk and implications for screening. Radiographics. 2015;35(2):302–15. https://doi.org/10.1148/rg.352140106.
42. Kuhl CK, Schrading S, Bieling HB, Wardelmann E, Leutner CC, Koenig R, et al. MRI for diagnosis of pure ductal carcinoma in situ: a prospective observational study. Lancet. 2007;11(9586):485–92. https://doi.org/10.1016/S0140-6736(07)61232-X.
43. Van Goethem M, Schelfout K, Kersschot E, Colpaert C, Weyler J, Verslegers I, et al. Comparison of MRI features of different grades of DCIS and invasive carcinoma of the breast. JBR-BTR. 2005;88(5):225–32. https://doi.org/10.1016/j.clinimag.2006.01.009.
44. Mann RM, Hoogeveen YL, Blickman JG, Boetes C. MRI compared to conventional diagnostic work-up in the detection and evaluation of invasive lobular carcinoma of the breast: a review of existing literature. Breast Cancer Res Treat. 2008;107(1):1–14. https://doi.org/10.1007/s10549-007-9528-5.

Authors and Affiliations

Gul Esen[1,2] · Deniz Esin Tekcan Sanli[3] · Sibel Kul[4] · Pinar Balci[5] · Nermin Tuncbilek[6] · Levent Celik[7] · Yasemin Kayadibi[8] · Ayse Nur Oktay Alfatli[9] · Serap Gultekin[10] · Fusun Taskin[1,2] · Mustafa Erkin Aribal[1,2] · Emel Ozveri[11] · Fatma Tokat[12] · Aykut Teymur[4] · Isil Basara Akin[5] · Gulsah Ozdemir[6] · Davut Can Guner[13] · Seda Aladag Kurt[8] · Ozge Aslan[9] · Aydan Avdan Aslan[10] · Ebru Yilmaz[14] · Yasemin Nur Icten[15,16] · Ahmet Necati Sanli[15]

✉ Deniz Esin Tekcan Sanli
tekcandenizesin@gmail.com

[1] Department of Radiology, Faculty of Medicine, Acibadem Mehmet Ali Aydınlar University, Istanbul, Turkey

[2] Senology Research Institute, Acibadem Mehmet Ali Aydınlar University, Istanbul, Turkey

[3] Department of Radiology, Faculty of Medicine, Gaziantep University, Gaziantep, Turkey

[4] Department of Radiology, Faculty of Medicine, Karadeniz Technical University, Trabzon, Turkey

[5] Department of Radiology, Faculty of Medicine, Dokuz Eylül University, Izmir, Turkey

[6] Department of Radiology, Faculty of Medicine, Trakya University, Edirne, Turkey

[7] Department of Radiology, Istanbul Oncology Hospital, Istanbul, Turkey

[8] Department of Radiology, Cerrahpasa Faculty of Medicine, Istanbul University-Cerrahpasa, Istanbul, Turkey

[9] Department of Radiology, Faculty of Medicine, Ege University, Izmir, Turkey

[10] Department of Radiology, Faculty of Medicine, Gazi University, Ankara, Turkey

[11] Department of General Surgery, Acibadem Kozyatağı Hospital, Istanbul, Turkey

[12] Department of Pathology, Acibadem Mehmet Ali Aydinlar University, Istanbul, Turkey

[13] Department of Radiology, Simav State Hospital, Kutahya, Turkey

[14] Department of Radiology, Acibadem Altunizade Hospital, Istanbul, Turkey

[15] Department of General Surgery, Abdulkadir Yüksel State Hospital, Gaziantep, Turkey

[16] Enka High School, Enka High School, Istanbul, Türkiye